SCIENCE CHINA
Information Sciences

• LETTER •

August 2025, Vol. 68, Iss. 8, 189301:1–189301:2
https://doi.org/10.1007/s11432-025-4447-2

A 40 μs latency cell-free mmWave reliable transmission experimental system via spatiotemporal 2-D coding

Ziyang ZHANG[1,2], Xiaohu YOU[1,2*], Dongming WANG[1,2*], Chuan ZHANG[1,2], Pengcheng ZHU[1,2], Jiaming LI[1,2], Yang CAO[1,2], Bin KUANG[2] & Qinji JIANG[1]

[1]*National Mobile Communications Research Laboratory, Southeast University, Nanjing 210096, China*
[2]*Purple Mountain Laboratories, Nanjing 211111, China*

Received 6 February 2025/Revised 28 April 2025/Accepted 14 May 2025/Published online 9 July 2025

Citation Zhang Z Y, You X H, Wang D M, et al. A 40 μs latency cell-free mmWave reliable transmission experimental system via spatiotemporal 2-D coding. Sci China Inf Sci, 2025, 68(8): 189301, https://doi.org/10.1007/s11432-025-4447-2

Implementation of spatiotemporal 2-D coding. The latency of the sixth-generation (6G) network is expected to be reduced from the ms scale in the existing fifth-generation (5G) network to the μs scale, to meet the demands of ultra-reliable and low-latency communication (uRLLC) requirements for extreme connectivity [1, 2]. The concept of spatiotemporal exchangeability and the spatiotemporal two-dimensional (2-D) coding was introduced in [3, 4]. These approaches mitigate the capacity collapse caused by limited temporal resources by enhancing spatial degrees of freedom (DoF) utilization. A closed-form expression of channel dispersion was analyzed in a massive multiple-input multiple-output (MIMO) system, further validating the spatiotemporal exchangeability theory [5]. Based on the above research and theoretical work, we conduct experimental evaluations of spatiotemporal 2-D coding for 6G extreme connectivity in multi-point-to-multi-point systems [6]. For single user massive MIMO systems, the spatial DoF remains constrained by the antenna number of the user equipment (UE). The current 5G new radio (NR) standard specifies a maximum of 8-layer transmission with two codewords for the single-UE [7], posing challenges for 2-D coding to utilize high spatial DoF. To address this limitation, we evolve the centralized 2-D coding to a cell-free distributed implementation, adopting the 2-D folding scheme in codeword trellis [4] as shown in Figure 1(a), and design the experimental system accordingly.

Experimental system. The cell-free distributed millimeter-wave (mmWave) experimental system consists of a baseband unit (BBU), prototype terminal, active antenna units (AAUs), and fronthaul cards, as illustrated in Figure 1(b). The AAUs on the BS and UE are connected to their respective BBU and prototype terminal via switches, enabling scalable AAU deployment. IEEE 1588 precision time protocol, a standard for a precision clock synchronization protocol, is used for the synchronization between the BBU and prototype terminal and AAUs [8]. The AAUs are deployed in a distributed configuration, and the experimental system adopts a cell-free transmission [6] and allows for scalable channel expansion and the waveform complies with 5G NR systems. To demonstrate the performance of 2-D coding, we only use two AAUs at BS and UE as depicted in Figure 1(c), and each AAU has two radio frequency chains with a dual-polarized phased array.

Scheduling analysis. The frame structure follows the 5G NR standard, with each slot configured as a mini-slot [7]. The first three orthogonal frequency-division multiplexing (OFDM) symbols on the BS are designated for downlink transmission, while the first three symbols on the UE are used for uplink reception. The remaining eleven OFDM symbols can be reserved for other user scheduling or services. The over-the-air (OTA) transmission spans two OFDM symbols, comprising one data and one demodulation reference signal (DMRS) symbol. In our evaluation, the AAU processing and the BBU receiving data require approximately one OFDM symbol period. Consequently, the physical (PHY) layer processing in uplink scheduling is delayed by three OFDM symbols, with a task chain latency of approximately two OFDM symbol periods. The scheduling process is depicted in Figure 1(d) and follows these steps.

Step 1. For UE reception, the uplink scheduling begins at the 13th OFDM symbol in the $(n-1)$-th slot. The BBU receives the media access control (MAC) scheduling information and starts tracking the end-to-end (E2E) latency of the PHY layer uplink task.

Step 2. The UE begins receiving and processing the data sent by BS in the n-th slot. Afterward, the AAU completes the processing, and the BBU reads the data.

Step 3. The UE starts symbol- and bit-level processing of the data at the 4th OFDM symbol in the n-th slot and obtains the cyclic redundancy check (CRC) result. All process repeats in each slot.

The BBU reads data and subsequently triggers the pro-

* Corresponding author (email: xhyu@seu.edu.cn, wangdm@seu.edu.cn)

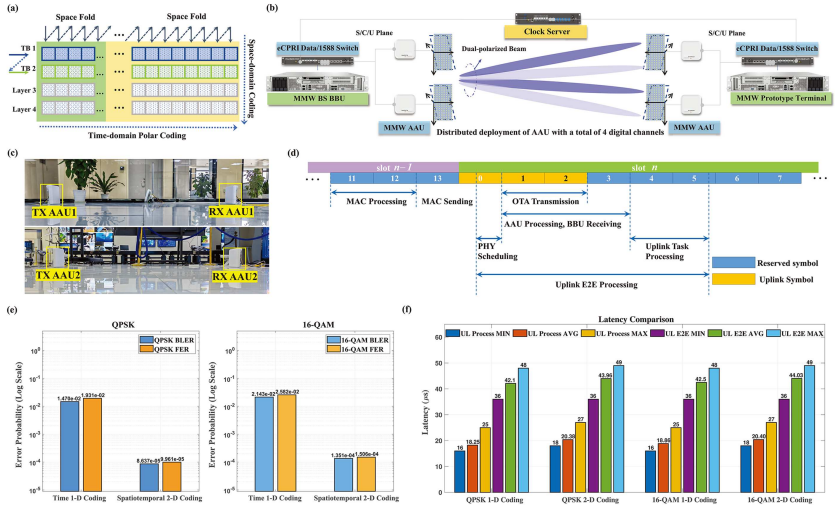

Figure 1 (Color online) (a) The diagram of the 2-D folding scheme; (b) transceiver architecture of the mmWave experimental system; (c) the system deployment; (d) slot scheduling process; (e) decoding reliability comparison; (f) uplink latency statistics comparison.

cessing chain until completion, which includes: resource configuration, resource element demapping, channel estimation, channel equalization, layer demapping, demodulation, deinterleaving, spatiotemporal 2-D decoding, and CRC checking.

Experimental result. We define the block error rate (BLER) and frame error rate (FER) of the coding as the CRC statistics for a transport block (TB) and the overall decoding statistics for all TBs, respectively. As shown in Figure 1(e), under the same channel conditions and spatiotemporal resources, the BLER and FER performance of spatiotemporal 2-D coding shows significant improvements compared to one-dimensional (1-D) temporal coding, i.e., traditional NR channel coding scheme. In finite block length scenarios, high-order modulation causes significant reliability degradation due to the capacity collapse effect, which can be effectively mitigated by introducing space-domain coding. Experimental results demonstrate that spatiotemporal 2-D coding offers a reliability gain of 2 to 3 orders of magnitude over 1-D temporal coding, without increasing the additional transmission OFDM symbol. More experiments can be found in Appendix A. The results in Figure 1(f) indicate that by adopting the special slot scheduling, the minimum uplink PHY layer E2E processing latency is less than 40 μs, representing one order of magnitude improvement over the 5G's latency. From Figure 1(f), we can observe that the system's processing latency and E2E latency remain stable under different modulation schemes. The average processing latency of spatiotemporal 2-D coding increases by approximately 2 μs compared to 1-D temporal coding, which is consistent with the result of expression (4) in [4]. This additional latency stems from the spatial encoding and folding processes and the extra complexity can be negligible with appropriate parallelization and vectorization in the experimental system. For more details, please refer to Appendix B.

Conclusion. Based on spatiotemporal exchangeability for uRLLC in extreme connectivity, we investigated the performance of spatiotemporal 2-D coding in a cell-free distributed mmWave MIMO-OFDM experimental system. Under the same channel conditions, spatiotemporal 2-D coding can effectively mitigate the capacity collapse effect in finite block length scenarios, achieving 2 to 3 orders of magnitude improvement in reliability. Additionally, through optimization of the special slot scheduling, the minimum uplink E2E latency was reduced to below 40 μs, representing an improvement of over one order of magnitude compared to 5G systems. These results validated the advantages of spatiotemporal 2-D coding, confirming its potential for a cell-free mmWave communication system, and providing a practical foundation for future extreme connectivity system design and deployment.

Acknowledgements This work was supported in part by National Key Research and Development Program of China (Grant No. 2021YFB2900300) and Jiangsu Science and Technology Major Project (Grant No. BG2024002).

Supporting information Appendixes A and B. The supporting information is available online at info.scichina.com and link.springer.com. The supporting materials are published as submitted, without typesetting or editing. The responsibility for scientific accuracy and content remains entirely with the authors.

References

1 You X H, Wang C X, Huang J, et al. Towards 6G wireless communication networks: vision, enabling technologies, and new paradigm shifts. Sci China Inf Sci, 2021, 64: 110301
2 Chen W S, Lin X Q, Lee J, et al. 5G-advanced toward 6G: past, present, and future. IEEE J Sel Areas Commun, 2023, 41: 1592–1619
3 You X H. 6G extreme connectivity via exploring spatiotemporal exchangeability. Sci China Inf Sci, 2023, 66: 130306
4 You X H, Zhang C, Sheng B, et al. Spatiotemporal 2-D channel coding for very low latency reliable MIMO transmission. In: Proceedings of IEEE Global Communications Conference (GLOBECOM), 2022
5 You X H, Sheng B, Huang Y M, et al. Closed-form approximation for performance bound of finite blocklength massive MIMO transmission. IEEE Trans Commun, 2023, 71: 6939–6951
6 Wang D M, You X H, Huang Y M, et al. Full-spectrum cell-free RAN for 6G systems: system design and experimental results. Sci China Inf Sci, 2023, 66: 130305
7 3GPP. Technical specification group radio access network. TS.38.211, TS.38.212. 2025. https://www.3gpp.org/ftp/Specs/archive/38_series
8 Murakami T, Aihara N, Tsukamoto Y, et al. Analysis of clock distribution in user-centric radio access network for cell-free massive MIMO. In: Proceedings of the 21st Consumer Communications & Networking Conference (CCNC), 2024